Pol. J. Environ. Stud. Vol. 32, No. 3 (2023), 2679-2688
DOI: *10.15244/pjoes/161437* ONLINE PUBLICATION DATE: 2023-04-06

Original Research

Experimental Investigation on the Association Between Diesel Exhaust Particulate Matter Exposure and Emphysematous Lungs: Airspace Enlargement of Alveolar Structures

Unggul Pundjung Juswono[1]*, Arinto Yudi Ponco Wardoyo[1], Johan Andoyo Effendi Noor[1], Arif Budianto[2]

[1]Physics Department, University of Brawijaya, Jl. Veteran 65145, Malang, East Java, Indonesia
[2]Physics Study Program, University of Mataram, Jl. Majapahit No. 62, Mataram, West Nusa Tenggara, Indonesia

Received: 13 August 2022
Accepted: 18 February 2023

Abstract

This study aimed to investigate the association between DEPs (diesel exhaust particulate matter) exposure and emphysematous lung. There were three buses used as diesel particulate matter sources. DEPs were classified into ultrafine, fine, and coarse particles with different aerodynamic diameters. This study used mice that were divided into control and treatment groups. The treated mice were exposed to the DEPs in different concentrations (low, mid, and high doses) for eight consecutive days. The control group did not receive any exposure treatment, while the exposed mice were sacrificed on the ninth day to get the lung samples. The lung samples were observed under a digital microscope to identify the normal and deformed alveolar cells. According to the observation results, the emphysematous level increased linearly to the DEPs dose concentration. The emphysematous level was found in the range of 64-80%, depending on the exposure dose concentration. In summary, direct exposure to the DEPs was correlated to the emphysematous level. This study has given a novel explanation of the bus exhaust emission risk as a heavy-duty vehicle in organs, especially due to the ultrafine, fine, and coarse particles exposures.

Keywords: alveolar cells, coarse particles, emphysema, fine particles, ultrafine particles

Introduction

The vehicular transportation sector has become a big concern now and is linked to air pollution due to the emissions of gaseous and particulate matter (PM). In terms of particulate emission, a previous study confirms that diesel engine vehicles emitted a huge amount of PMs with different diameters [1]. Another scenario in Los Angeles, United States, shows that the areas inside and outside buses had high ultrafine particle (UP or $PM_{0.1}$) concentrations with a concentration of more than 100,000 particles/cm^3 [2]. The bus also emits

*e-mail: unggul-pj@ub.ac.id

a bigger PM, with a different particle size distribution, including fine particles (particulate matter with a diameter less than 2.5 μm, FP or $PM_{2.5}$) and coarse particles (particulate matter with a diameter less than ten μm, CP or PM_{10}).

A previous study has shown that PM from many combustion sources can affect human health. Due to the smallest size, UPs have a great deposition efficiency in the organ [3]. As described in a previous study, exposures to UPs from indoor and outdoor sources have been associated with the altered level of the endothelial progenitor cell and might adversely affect human vascular health [4]. In an experimental animal, such effects on health can be compared with cell deformation effects resulting from short-term to long-term exposure to UPs [5]. Exposure to the UPs with a certain concentration has been related to decreasing platelets and polymorphonuclear leukocytes [6]. In terms of lung health modeling due to dust level, the increasing amount of dust levels increases lung cancer risk [7]. For the bigger diameter size of particulate matters, there was reported that there is a significant correlation between the increase of daily FPs concentration and lung cancer possibility, in which the incidence rate of lung cancer increased by 36% for the increasing amount of daily FPs concentration of 10 ug/m^3. Another study also concerns PMs' toxicity for the lungs, reviewing the association of indoor FPs from environmental tobacco smoke and chronic lung diseases [8].

There are many studies that state and confirm the composition of diesel exhaust particles. Mostly, they consist of PAHs (polycyclic aromatic hydrocarbons) and VOCs (volatile organic compounds), also semi-volatile and volatile PAHs [9-13]. On the other hand, it needs more novelty in understanding PM emission characterization in health impacts. Many studies have been conducted to characterize diesel exhaust emissions [9, 10]. Many literature reviews show a gap in understanding diesel exhaust particles' impact on health, especially in lung cells, due to exposure to diesel bus exhaust emission. Our previous research using red blood cells and kidney cells has confirmed the deformation levels due to UP exposure [5, 14]. In contrast, information about the impact of FP and CP emitted from a heavy-duty diesel engine is unavailable. As consecutive research and a better understanding of the PM's negative impact on health, it is necessary to examine the impact on the lung cells, with a common emission source in some countries, such as diesel engine buses.

Experimental

Bus Samples

Three diesel engine buses (B1 (cylinder volume = 6,728 cm^3), B2 (cylinder volume = 7,961 cm^3), and B3 (cylinder volume = 4,214 cm^3)) that were appropriately maintained and inspected were used as the emission sources. They had no mechanical problems and were parked outdoors not longer than 12 hours after leaving the garages.

Animals

One hundred fifty male mice (20-23 g BW), aged ten weeks, were obtained from Brawijaya University, Indonesia. They were housed in natural illumination, 12 hours/ dark-light cycle, controlled room temperature (25±1ºC), and provided with food and water *ad libitum*. The mice had three days of acclimatization prior to the exposure treatments. Afterward, they were randomly divided into the Control, UP, FP, and CP groups (Table 1). All procedures were approved by the Animal

Table 1. The scheme of the control and exposure groups (n = 5 per group).

Exposure Groups	Bus Samples	Smoke Injection Times (seconds)	Number of Mice	Subgroup Codes
Control (CTRL)	-	Unexposed	5	UP_0
	-	Unexposed	5	FP_0
	-	Unexposed	5	CP_0
Ultrafine particles (UP)	B1	20; 40; 60	5; 5; 5	$UPB1_{20}$; $UPB1_{40}$; $UPB1_{60}$
	B2	20; 40; 60	5; 5; 5	$UPB2_{20}$; $UPB2_{40}$; $UPB2_{60}$
	B3	20; 40; 60	5; 5; 5	$UPB3_{20}$; $UPB3_{40}$; $UPB3_{60}$
Fine particles (FP)	B1	20; 40; 60	5; 5; 5	$FPB1_{20}$; $FPB1_{40}$; $FPB1_{60}$
	B2	20; 40; 60	5; 5; 5	$FPB2_{20}$; $FPB2_{40}$; $FPB2_{60}$
	B3	20; 40; 60	5; 5; 5	$FPB3_{20}$; $FPB3_{40}$; $FPB3_{60}$
Coarse particles (CP)	B1	20; 40; 60	5; 5; 5	$CPB1_{20}$; $CPB1_{40}$; $CPB1_{60}$
	B2	20; 40; 60	5; 5; 5	$CPB2_{20}$; $CPB2_{40}$; $CPB2_{60}$
	B3	20; 40; 60	5; 5; 5	$CPB3_{20}$; $CPB3_{40}$; $CPB3_{60}$

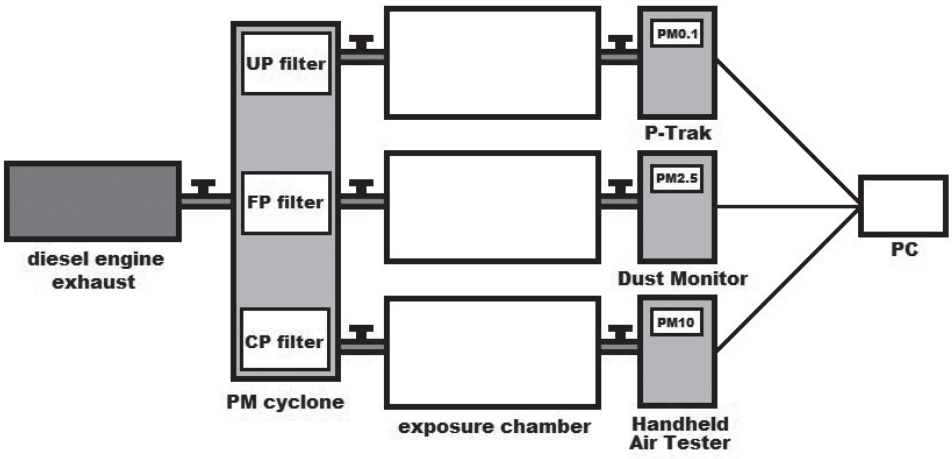

Fig. 1. DEPs measurement setup inside the exposure chambers.

Care and Use Committee of Brawijaya University (Number: 541-KEP-UB).

Preparation of DEPs

The diesel bus exhaust emission was introduced to a PM cyclone containing an N95 particulate respirator (3M, Model 8210), Whatman filter papers (Grade 42 and Grade 40), a suction pump (flow rate = 2.03 m/s), valve, and a cylindrical tube (diameter: 7.62 cm) (Fig. 1) for 20, 40, and 60 seconds to generate three different PM concentrations: C1 (low concentration, 20 seconds), C2 (medium concentration, 40 seconds), and C3 (high concentration, 60 seconds) in three different diameters (UP, FP, and CP) [15, 16]. This cyclone was also tested using a HEPA filter. Based on our preliminary studies, the mice collapsed for the given DEPs by the injection time for more than 60 seconds. Thus, the injection times were divided into those selected times. The concentration of the UPs was measured using a P-Trak Ultrafine Particle Counter (TSI, model 8525) with the measured diameter range of 0.02-0.1 μm [17]. A Digital Dust Monitor (Kanomax, model 3443) was used to measure filtered FP concentrations (diameter range of 0.1-2.5 μm). The biggest PM generated by the cyclone (diameter range 2.5-8 μm), CPs, was monitored using a Handheld Air Tester (Hinaway, model CW HAT200S). The total concentration of the DEPs was obtained by summing the measured concentrations [18].

Animal Treatment

According to Table 2, the mice from each group were exposed to a certain dose of DEPs. For example, the mice from $UPB1_{20}$, $UPB1_{40}$, and $UPB1_{60}$ subgroups were exposed to filtered UPs emitted by B1 for 20,

Table 2. The number of normal and emphysematous cells of mice.

Groups	Subgroups	B1		B2		B3	
		EC	Normal	*EC*	Normal	*EC*	Normal
CP	CP_0	2±1	25±7	2±1	25±7	2±1	25±7
	20 s	21±4	15±6	13±3	7±2	12±4	6±3
	40 s	15±2	10±4	22±3	10±4	17±1	7±1
	60 s	14±5	7±3	12±5	5±2	14±1	5±1
FP	FP_0	2±1	26±9	2±1	26±9	2±1	26±9
	20 s	20±4	11±4	28±2	15±4	26±9	12±3
	40 s	21±3	10±4	35±4	17±7	22±7	10±4
	60 s	32±3	14±4	21±11	8±3	27±2	12±2
UP	UP_0	2±1	35±8	2±1	35±8	2±1	35±8
	20 s	28±4	13±3	28±3	13±3	22±3	9±2
	40 s	20±2	7±3	25±3	9±3	20±6	7±1
	60 s	28±2	9±2	26±3	9±4	26±4	7±2

40, and 60 seconds consecutively. Similar treatments were also applied to the other bus samples, B2 and B3. The mice from the FP group were exposed to FP emitted by B1, B2, and B3 with the selected times: 20 ($FPB1_{20}$, $FPB2_{20}$, and $FPB3_{20}$), 40 ($FPB1_{40}$, $FPB2_{40}$, and $FPB3_{40}$), and 60 seconds ($FPB1_{60}$, $FPB2_{60}$, and $FPB3_{60}$). Similar to these, The mice from the CP group were exposed to CP with the selected times: 20 ($CPB1_{20}$, $CPB2_{20}$, and $CPB3_{20}$), 40 ($CPB1_{40}$, $CPB2_{40}$, and $CPB3_{40}$), and 60 seconds ($CPB1_{60}$, $CPB2_{60}$, and $CPB3_{60}$). After that, the mice were penned inside the exposure chamber (20 cm of width x 30 cm of length x 20 cm of height) for 100 seconds for the inhalation procedure. These treatments were conducted for all subgroups on eight consecutive days (once exposure per day). The selected inhalation time and the number of exposure days were prior to our preliminary studies to prevent collapsed mice due to longer treatment time [5, 14].

Histological Studies

All mice were sacrificed using a cervical dislocation method on the 9th day after the sequence exposures for eight days. The lung samples were prepared for the paraffin sections. They were fixed in the buffered formalin (10%). Formalin-fixed tissue was embedded in the paraffin and sectioned at 5 um thickness. HE (hematoxylin and eosin) staining was used to examine the lungs. The rest organs were excised. The prepared sample's slides were observed under a digital microscope (500x magnification) laying on twenty-five random fields by an experienced pathologist [19]. For the possibility of particulate deposition investigation, the sample sections were placed on the carbon discs and spatter-coated [19]. These sections were examined using a scanning electron microscope (SEM, Phenom). The examinations were obtained in randomly selected five fields at 2000x magnification (15.00 kV). The deformed cells percentage is obtained by calculating the number of normal and deformed cells. Thus, the emphysematous level (*El*) of the alveolar cells is determined as the ratio of the emphysematous cells (*EC*) versus the total alveolar cells (*AC*) calculated from the digital images, as seen below:

$$\%El = \frac{EC}{AC}\ x\ 100\% \tag{1}$$

Statistical Analysis

All results are expressed as the mean±standard deviation (SD) from three (particle concentration measurements), five (treated mice), and twenty-five (random fields) independent experiments. A significant difference between groups was performed by the Student's *t*-test (a probability level of $p<0.05$ indicates a significant difference). The correlation between the DEP concentration and the emphysema level was evaluated by a logarithmic regression test, in which $R^2>0.90$ indicates a high correlation [15, 16].

Results

DEP Concentrations

In this study, DEPs concentrations data collection was conducted for three diesel engine buses on the eight exposure days. The results are shown in Fig. 2. According to the results, the DEPs concentrations are heterogeneous in UP, FP, and CP concentrations. As shown in the figure, there is a significant difference between B1, B2, and B3, indicating different buses impacted the emissions characteristics ($p<0.05$).

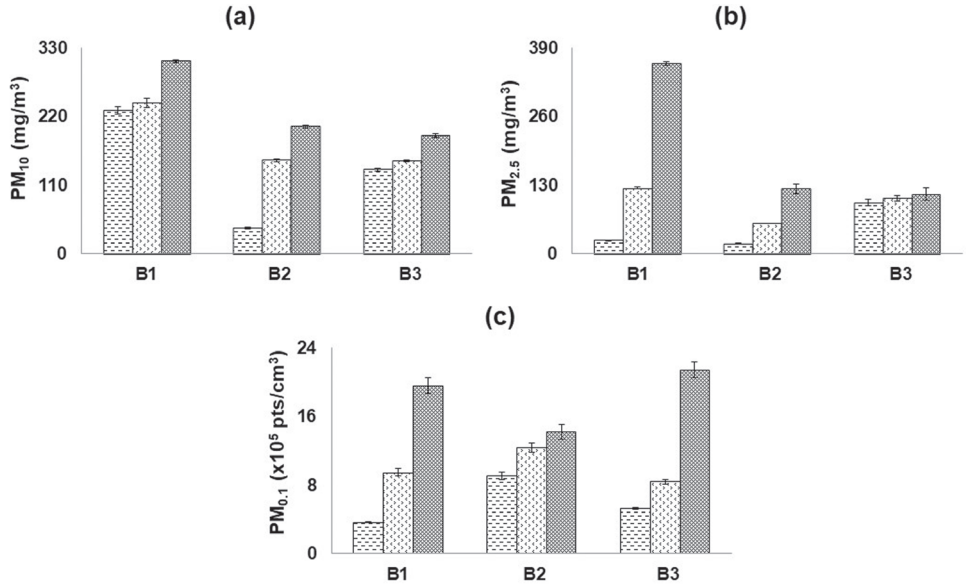

Fig. 2. The total concentrations of DEPs exposed to the mice for eight consecutive days: a) CPs; b) FPs; and c) UPs.

This situation occurs in all injection times (20, 40, and 60 seconds). B3 has the most UP concentration (21.45 x 10^5 particles/cm^3) compared to the results obtained in B1 (19.57 x 10^5 particles/cm^3) and B2 (14.19 x 10^5 particles/cm^3) for 60 seconds of injected time. On the second injected time, 40 seconds, the highest UP concentration is found in B2 (12.36 x 10^5 particles/cm^3). This value is higher than B1 (9.47 x 10^5 particles/cm^3) and B3 (8.40 x 10^5 particles/cm^3) of the 40 seconds of the injected time. Interestingly, B2 also dominates the concentration of the UPs on the 20 seconds of injected time, resulting in 9.08 x 10^5 particles/cm^3. B1 and B3 only have 3.68 x 10^5 particles/cm^3 and 5.27 x 10^5 particles/cm^3.

B1 dominates FP concentrations on the medium diameter class on the 40 and 60 seconds of injected times, 124 mg/m^3, and 360 mg/m^3. These values are higher than the values of B2 (57 mg/m^3 and 123 mg/m^3) and B3 (105 mg/m^3 and 113 mg/m^3). On the 20 seconds of injection time, B2 and B3 have 19 mg/m^3 and 97 mg/m^3 of FP concentrations; meanwhile, 25 mg/m^3 is found in B1.

B1 generates the highest CP concentrations for all injected times: 230 mg/m^3, 242 mg/m^3, and 309 mg/m^3, consecutively for 20, 40, and 60 seconds of injected times. The CP concentrations of B2 are different from B1, showing 41 mg/m^3, 150 mg/m^3, and 204 mg/m^3, consecutively for 20, 40, and 60 seconds of injection times. The different results are also found in B3, having 135 mg/m^3, 149 mg/m^3, and 189 mg/m^3, respectively, for 20, 40, and 60 seconds of injection times.

Histological Examinations

The statistical analysis compares differences in emphysematous alveolar cells of UPs, FPs, and CPs. According to the histological examination, the statistical test result shows a significant difference between the levels of emphysematous alveolar cells calculated in the groups of UP, FP, and CP (since $p<0.05$). This result also indicates that each PM diameter gives different health impacts in deforming alveolar structures.

The histological examination of the alveolar cells showed normal and abnormal cells (Fig. 3). The identified emphysematous cells were found as acute enlargement of the wall structure. The emphysematous alveolar cells had acute morphological changes (enlargement) in the alveolar cell's airspace (indicated by the blue lines), which had the potential to induce emphysema. The green circles show normal alveolar cells, having no inflammatory and degenerative cases [20, 21]. According to the histopathological examination results, the lowest concentrations of the UPs have the most normal cells, whether in B1, B2, or B3. The number of emphysematous cells in all groups is higher than normal cells. Meanwhile, the mice from the CTRL groups CP_0, FP_0, and UP_0 did not show any noticeable alterations in alveolar cell deformability than the

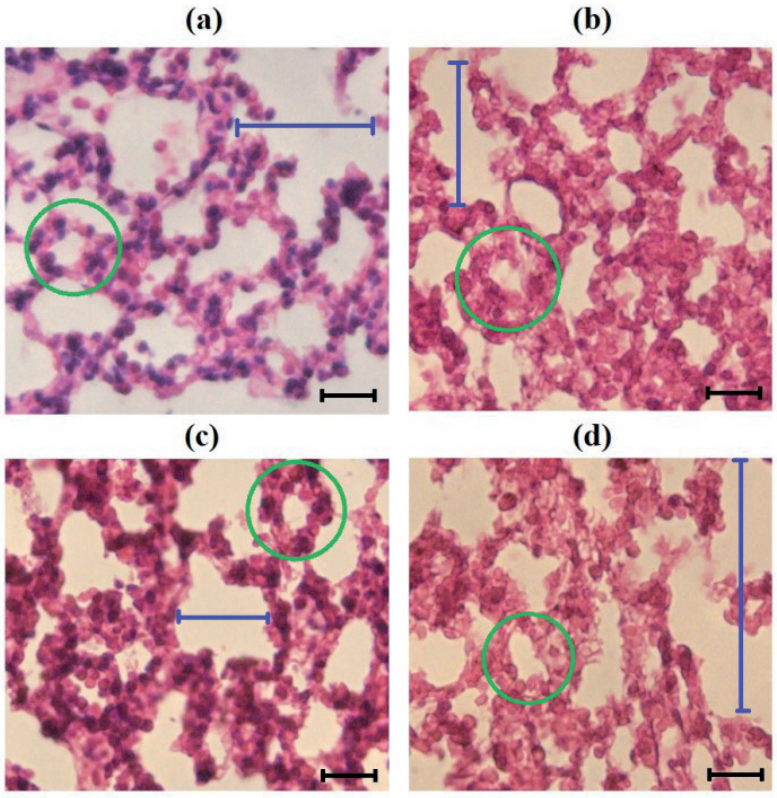

Fig. 3. The normal and emphysematous cells in the lung of mice treated for eight consecutive days with the dose of high concentrations C3 for: a) control group; b) ultrafine particle; c) fine particles; and d) coarse particles (scale bars = 20 μm).

exposed mice from CP, FP, and UP groups. All results are interpreted in Table 2.

Deformation Level versus DEPs' Concentration

In this regard, we found that exposures to CPs with a diameter <10 μm significantly correlated to emphysematous cell's level. As seen in Fig. 4(a-c), the correlation between them are interpreted as the R^2>0.80 (R^2 value are 0.99, 0.98, and 0.89, respectively, for B1, B2, and B3). C3, as the highest dose of CP concentrations, has 60%, 64%, and 67% of emphysematous levels, respectively, for B1, B2, and B3. These values are higher than the emphysematous levels obtained in $CPB1_2$-$CPB1_{40}$ (51% and 53%) and $CPB2_{20}$ and $CPB2_{40}$ (58% and 62%). Moreover, these results demonstrate that C3 may cause a higher inflammatory response due to exposure to CPs, compared to C1 and C2.

Similarly, as shown in Fig. 5(a-c), the exposed FPs, which have a smaller diameter, cause 58%, 61%,

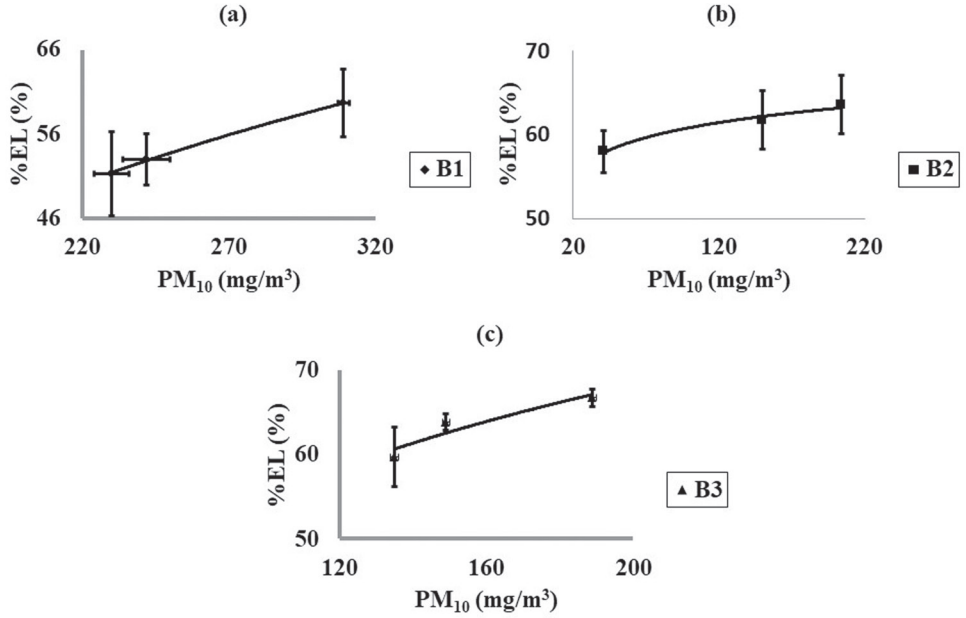

Fig. 4. The correlation between coarse particles concentration and the emphysematous cells of mice's lungs: a) B1; b) B2; and c) B3 (R^2>0.80).

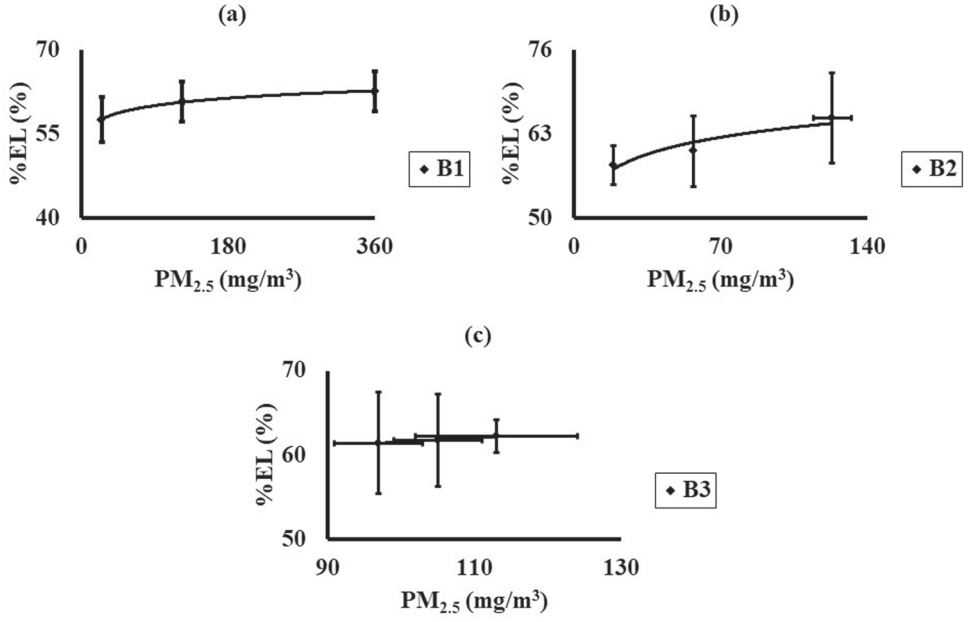

Fig. 5. The correlation between fine particles concentration and the emphysematous cells of mice's lungs: a) B1; b) B2; and c) B3 (R^2>0.80).

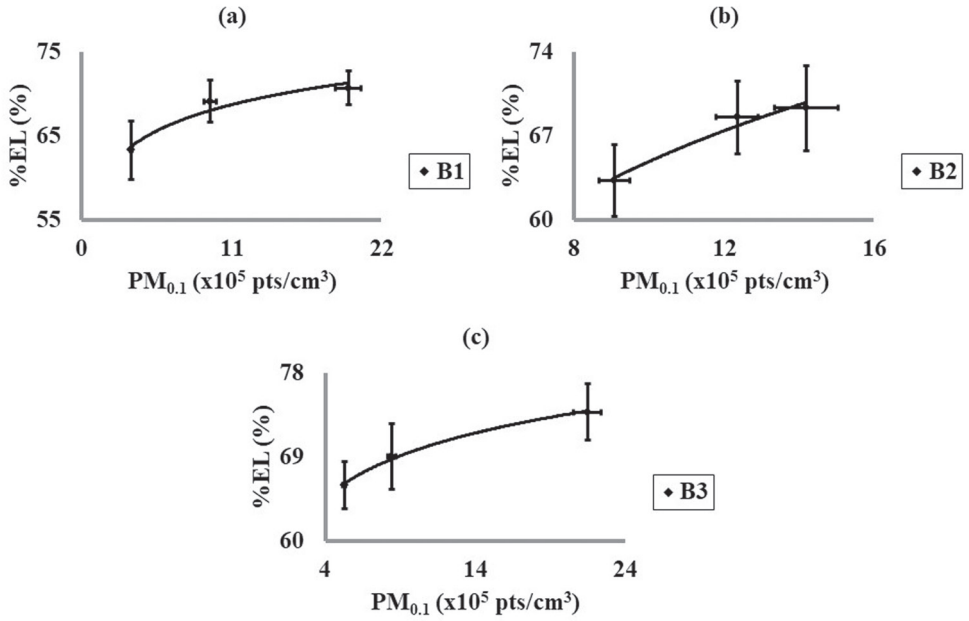

Fig. 6. The correlation between ultrafine particles concentration and the emphysematous cells of mice's lungs: a) B1; b) B2; and c) B3 (R^2>0.90).

and 63% of an emphysematous level, respectively $FPB1_{20}$, $FPB1_{40}$, and $FPB1_{60}$. B2 subgroup has 58% (C1), 60% (C2), and 65% (C3) of emphysematous levels, a little higher than the B1 subgroup. Another bus sample, B3, shows a similar trendline, with the amount of 61% (C1), 62% (C2), and 62% (C3), resulting in an R^2 value of 0.98.

Then, UP (diameter range 0.02-0.1 μm) analysis shows that the emphysematous level was further increased by the smallest diameter than the results obtained in CP and FP groups (Fig. 6a-c). $UPB1_{60}$ treatment significantly annotates the emphysematous level of the mice's lungs (71%), compared to $UPB1_{20}$ (63%) and $UPB1_{40}$ (69%). These treatments correlate well to the dose of UPs exposed to the mice, resulting in R^2 = 0.94. Another bus sample was used to confirm the potential health impact of UPs exposure, B2. Consistently, the B2 subgroup shows similar effects as B1, resulting in 63% (C1), 69% (C2), and 69% (C3) of emphysematous levels (R^2 = 0.96). Another bus sample, B3, shows a similar trendline, with the amount of 66% (C1), 69% (C2), and 74% (C3), resulting in an R^2 value of 0.99.

Moreover, UP, FP, and CP's effects on the deformation of the alveolar cells were assessed using three different bus samples. There is a significant difference between UP, FP, and CP results. Results obtained with FP were similar to CP. For CP, only slight toxicity was noted. Compared to the smallest particles, CP has the least emphysematous level. These results indicate that exposure to smaller particles results in higher toxicity. In contrast, no effect on alveolar cells nor any cell mortality was observed in CTRL.

Discussion

Diesel exhaust particles, DEPs, are recognized as a critical health problem because of their toxicity. They can easily enter the respiratory area and may cause negative impacts. It is very important to characterize and reduce exhaust emissions. However, many conducted studies investigate these topics, giving great information and a better understanding of diesel exhaust particle emissions. Besides, the current harmful impacts of DEPs on health cannot be ignored. Therefore, this study examined the correlation between DEPs exposure concentration and the emphysematous lungs of mice. As interpreted in the results, the study reports that exposing the mice to DEPs emitted from diesel engine buses resulted in alveolar cell deformation. This study also alleviates the levels obtained from each exposure subgroup with the values obtained in the control groups to correlate the exposure to DEPs and the emphysematous level. As expected, a significant correlation between the exposed DEPs and the emphysematous levels on B1 is indicated by a logarithmic trendline, with an R^2 value>0.90 for ultrafine, fine, and coarse particle groups. Similar results are shown by B2 and B3, as interpreted in Figs 4-6. No significant differences are found in B1, B2, and B3 results. All results give the R^2 values>0.80. These results indicate that significant emphysema level increases occurred in the treatment groups' alveolar cells but not in the control group. These correlations are well confirmed by our previous study using motorcycle exhaust emissions in the erythrocytes and tubular epithelial cells [5, 14].

Interestingly, the exposure effects of DEPs are also associated with particle toxicity and the cell reaction (inflammation) with the toxic agent, including the particle size variation [22]. According to the results, UPs have the most emphysematous level compared to FPs and CPs. In other words, exposure to the smallest particles causes more toxicity in inducing cell deformation. CPs indeed have the smallest emphysematous level. Furthermore, these results indicate that CP can still deposit deeper in the respiratory area. It means that CPs still can pass through the upper filter of the respiratory area, causing tissue inflammation, and our results are consistent with the previous study with a diameter <10 µm [23].

A possible mechanism of these inflammatory responses is the deposition ability of DEPs in the respiratory area. Due to the PMs' high deposition capability (especially for the UPs, as the smallest particulate matter) in the lung, these particles induced the lung before following the bloodstream to the deeper organs, as the first possible mechanism of the particulate matter toxicity in organs. After deposited, they might have more chance to activate the inflammatory cells [24], inducing oxidative stress [4]. As confirmed in the previous study, the deposited particles-inducing cell activation might induce pro-inflammatory cytokines and generate more free radicals in the body [23]. The reactions then trigger the chain reactions, including inflammation, allergy, tissue damage, and airway obstruction [21, 24], in which the level of the inflammatory responses due to the possible change in free-radical composition might relate to the particulate matter toxicity. This particle infiltration then contributed to pathogenesis in the respiratory area and released proinflammatory cytokines [24, 25].

As reported by the previous studies, the respiratory tract's inflammation was related to particle deposition [26]. According to the modeling study about the particle deposition in the respiratory tract [3], it seems that the inhaled PMs deposited in the lung and altered the alveolar cell shape directly. This study also identified some substances with different shapes according to the normal alveolar cells based on the histopathological examination. These expected particles were distinguished according to the shape and wall structure differences compared to the normal alveolar cells in the exposed and unexposed mice. We identified these abnormal substances in electron micrographs (2500x of magnification). In contrast, there were no abnormalities in the surface, and no abnormal substances were observed in the control groups. Meanwhile, there were some abnormal substances in the exposed mice as identified as the submicron particles with a diameter <0.1 µm or UPs (blue circles) and >0.1 µm as the agglomerated FPs (Fig. 7).

As it is interpreted in Fig. 7, this study confirmed the existence of inflammation in the alveolar cells

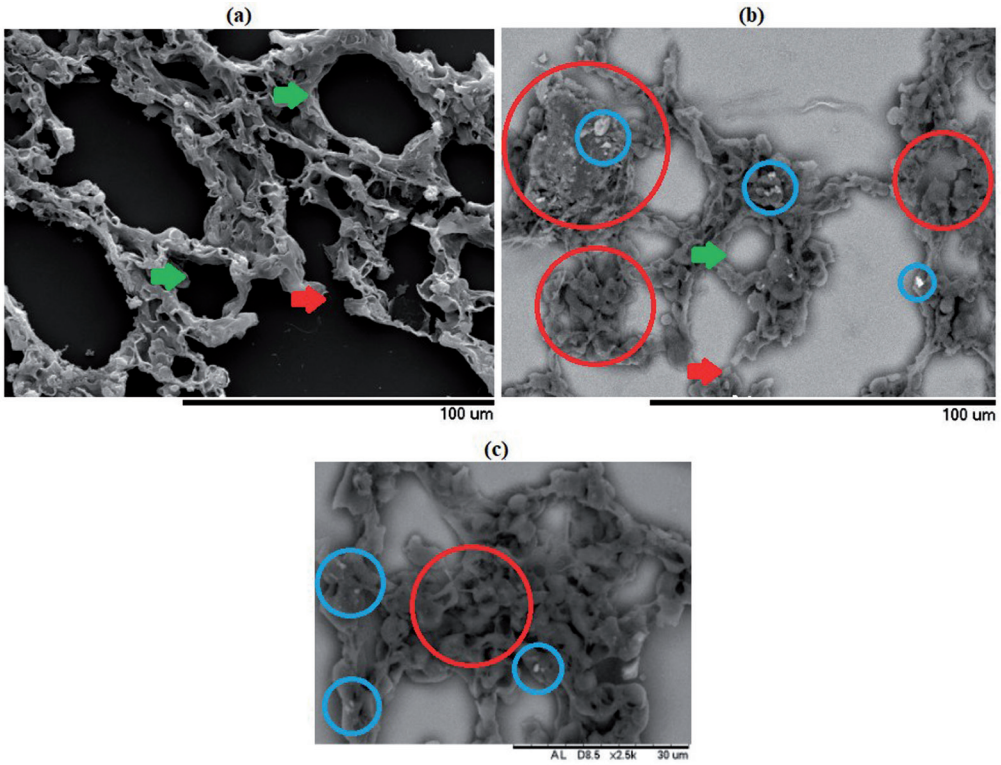

Fig. 7. Scanning electron images of alveolar cells: (a) control (scale bar 100 µm); (b-c) Mice exposed to C3 of ultrafine particles (scale bars 100 µm and 30 µm). Green arrows indicate normal alveolar cells. Red arrows show disruption of the alveolar wall structure. Red circles indicate an inflammation related to cell adaptation.

that might relate to the alveolar deformation, as well as the emphysema. The previous study's result also supported this expected result, showing the high correlation between the alveolar cells' inflammation and emphysema. As the chain reaction, the inflammation triggered other responses to counterbalance free radical particulate matters and oxidant production and generated ROS (Reactive Oxygen Species) [4]. The increasing amount of ROS due to the toxic agents was associated with oxidative stress and the activation and injury of the respiratory tract cells [24, 25]. Under normal conditions, the body's defense system will generate something to deal with oxidative stress and inflammation due to ROS generation. The body system might also alleviate acute lung injury by restraining the activation of NF-κB (nuclear factor- κB) and MAPKs (mitogen-activated protein kinases) [27]. The body's immune system will reduce ROS and prevent cellular dysfunction and apoptotic or cell death. However, when the level of ROS (i.e., H_2O_2) exceeds the antioxidant ability, there will be this oxidative stress.

The different results indicate that exposure to DEPs has a significant correlation with the deformed cells as an inflammatory response due to the exposed particles' chemical compounds. As stated in the previous studies, diesel engine emissions consist of PMs with many chemical compounds, such as VOCs, PAHs, semi-volatile PAHs, non-volatile PAHs, and several organic-inorganic compounds [28, 29]. PAHs and VOCs are known as hazardous materials for human health due to their carcinogenic and mutagenic characteristics [30, 31]. Other studies revealed that PAHs are well-known toxic to humans and related to Alzheimer's disease [32]. Other diesel exhaust particle characterizations show the existence of alkanes and alkenes [11] and C_{24} to C_{32} organic compounds, indicating an unburned oil [1].

Conclusions

In summary, diesel exhaust emissions can generate coarse, fine, and ultrafine particles. The exposure to the diesel exhaust particles from all bus samples caused emphysematous alveolar cells in the mice's lungs (R^2>0.80). The most acute physical damage in alveolar cells is obtained at the $PM_{0.1}$ or UP (ultrafine particle) group with the least particle diameter. These effects suggest acute physical damage in alveolar cells determined by the enlargement of the lung's airspaces, including the destruction of the tissues surrounding the airspace walls, compared to the normal ones. The emphysematous lungs' level was related to the exposed particles, in which a smaller diameter causes more damage. This study may better explain the risk of bus emission as a heavy-duty motor vehicle that is high risk in the organ.

Acknowledgments

The authors wish to acknowledge Eko T.P. Adi, Mia A. Pawestri, and Arsyal K. Rumpoko for their excellent technical assistance.

Conflict of Interest

The authors declare no conflict of interest.

References

1. SAKURAI H., TOBIAS H.J., PARK K., ZARLING D., DOCHERTY K.S., KITTELSON D.B., MCMURRY P.H., ZIEMANN P.J. On-line measurements of diesel nanoparticle composition and volatility. Atmos. Environ., **37**, 1199, **2003**.
2. ZHANG Q., FISCHER H.J., WEISS R.E., ZHU Y. Ultrafine particle concentrations in and around idling school buses. Atmos. Environ., **69** (2), 65, **2013**.
3. ASGHARIAN B, MILLER F.J., PRICE O., SCHROETER J.D., EINSTEIN D.R., CORLEY R.A., BENTLEY T. Modeling particle deposition in the pig respiratory tract. J Aerosol Sci., **99**, 107, **2016**.
4. JANTZEN K., MØLLER P., KAROTTKI D.G., OLSEN Y., BEKÖ G., CLAUSEN G., HERSOUG L.G., LOFT S. Exposure to ultrafine particles, intracellular production of reactive oxygen species in leukocytes and altered levels of endothelial progenitor cells. Toxicology, **359**, 11, **2016**.
5. WARDOYO A.Y.P., JUSWONO U.P., NOOR J.A.E. Varied dose exposures to ultrafine particles in the motorcycle smoke cause kidney cell damages in male mice. Toxicol. Reports, **5**, 383, **2018**.
6. BRÜSKE I., HAMPEL R., SOCHER M.M., RÜCKERL R., SCHNEIDER A., HEINRICH J., OBERDÖRSTER G., WICHMANN H.-E., PETERS A. Impact of ambient air pollution on the differential white blood cell count in patients with chronic pulmonary disease. Inhal. Toxicol., **22** (3), 245, **2010**.
7. JENWITHEESUK K., PEANSUKWECH U., JENWITHEESUK K. Construction of polluted aerosol in accumulation that affects the incidence of lung cancer. Heliyon, **6** (2), e03337, **2020**.
8. NI Y., SHI G., QU J. Indoor $PM_{2.5}$, tobacco smoking and chronic lung diseases: A narrative review. Environ. Res., **181** (November), 108910, **2020**.
9. YANG Z, LIU Y, WU L, MARTINET S, ZHANG Y, ANDRE M, MAO H. Real-world gaseous emission characteristics of Euro 6b light-duty gasoline- and diesel-fueled vehicles. Transp. Res. Part D Transp. Environ., **78**, 102215, **2020**.
10. LIN Y.C., LI Y.C., AMESHO K.T.T., CHOU F.C., CHENG P.C. Characterization and quantification of $PM_{2.5}$ emissions and PAHs concentration in $PM_{2.5}$ from the exhausts of diesel vehicles with various accumulated mileages. Sci. Total Environ., **660**, 188, **2019**.
11. YAO Z., SHEN X., YE Y., CAO X., JIANG X., ZHANG Y., HE K. On-road emission characteristics of VOCs from diesel trucks in Beijing, China. Atmos. Environ., **103**, 87, **2015**.
12. WANG M., LI S., ZHU R., ZHANG R., ZU L., WANG Y., BAO X. On-road tailpipe emission characteristics

and ozone formation potentials of VOCs from gasoline, diesel and liquefied petroleum gas fueled vehicles. Atmos. Environ., **223**, 1, **2020**.
13. SLEZAKOVA K., CASTRO D., DELERUE C., ALVIM C., MORAIS S., PEREIRA C. Impact of vehicular traffic emissions on particulate-bound PAHs: Levels and associated health risks. Atmos. Res., **127**, 141, **2013**.
14. WARDOYO A.Y.P., JUSWONO U.P., NOOR J.A.E. A study of the correlation between ultrafine particle emissions in motorcycle smoke and mice erythrocyte damages. Exp Toxicol. Pathol., **69**, 649, **2017**.
15. BUDIANTO A., WARDOYO A.Y.P., MASRUROH, DHARMAWAN H. A. An airborne fungal spore mass measurement system based on graphene oxide coated QCM. Pol. J. Environ. Stud., **31** (4), 3523, **2022**.
16. HADI K.A., WARDOYO A.Y.P., JUSWONO U.P., NABA A., BUDIANTO A., ADI E.T.P. A study of erythrocyte deformation level related to biomass burning emission exposures using artificial neural networks. Pol. J. Environ. Stud., **31** (6), 5037, 2022.
17. WARDOYO A.Y.P., JUSWONO U.P., VALENTINO A., HUDA F.B. Quantification of ultrafine particle emission factors from motor bikes. Int. J Appl. Eng. Res., **10** (19), 40276, **2015**.
18. WARDOYO A.Y.P., MORAWSKA L., RISTOVSKI Z.D., MARSH J. Quantification of particle number and mass emission factors from combustion of Queensland trees. Environ. Sci. Technol. Technol., **40** (18), 5696, **2006**.
19. TSUCHIYA K., INASE N., ICHINOSE S., USUI Y., MIYAZAKI Y., OHTANI Y., ANDO N., AKASHI T., KONDOH Y., TANIGUCHI H., YOSHIZAWA Y. Elemental analysis of inorganic dusts in lung tissues of interstitial pneumonias. J Med. Dent. Sci., **54** (1), 9, **2007**.
20. INOUE K., KOIKE E., TAKANO H. Comprehensive analysis of elastase-induced pulmonary emphysema in mice: Effects of ambient existing particulate matters. Int. Immunopharmacol., **10** (11), 1380, **2010**.
21. HUSSAIN A.F., SULAIMAN G.M., DHEEB B.I., HASHIM A.J., ALRAHMAN E.S.A., SEDDIQ S.H., KHASHMAN B.M. Histopathological changes and expression of transforming growth factor beta (TGF-β3) in mice exposed to gliotoxin. J King Saud. Univ – Sci., **32** (1), 716, **2020**.
22. ZAKHARENKOA A.M., ENGIN A.B., CHERNYSHEVA V.V., CHAIKAA V.V., UGAYA S.M., REZAEE R., KARIMI G., DROZD V.A., NIKITINA A.V., SOLOMENNIK S.F., KUDRYAVKINA O.R., XIN L., WENPENG Y., TZATZARAKIS M., TSATSAKIS A.M., GOLOKHVAST K.S. Basophil mediated pro-allergic inflammation in vehicle-emitted particles exposure. Environ. Res., **152**, 308, **2017**.
23. PIAO Z., YOO J.K., PARK B.W., SEO S.B., PARK S.J., JEON H.Y., RAHMAN M.M., KIM N., KIM S. Therapeutic effects of shibashin misena® against fine-dust-induced pulmonary disorders in mice. Biomed. Pharmacother., **125**, 110018, **2020**.
24. KREYLING W.G., SEMMLER M., MÖLLER W. Dosimetry and toxicology of ultrafine particles. J Aerosol Med., **17** (2), 140, **2004**.
25. EUN K., CHO D., JEONG H. Air pollution and skin diseases: Adverse effects of airborne particulate matter on various skin diseases. Life Sci., **152**, 126, **2016**.
26. ORAVISJÄRVI K., PIETIKÄINEN M., RUUSKANEN J., NIEMI S., LAURÉN M., VOUTILAINEN A., KEISKI R.L., RAUTIO A. Diesel particle composition after exhaust after-treatment of an off-road diesel engine and modeling of deposition into the human lung. J Aerosol. Sci., **69**, 32, **2014**.
27. LIU H., LIN Z., MA Y. Suppression of Fpr2 expression protects against endotoxin-induced acute lung injury by interacting with Nrf2-regulated TAK1 activation. Biomed. Pharmacother., **125** (January), 109943, **2020**.
28. SEIGNEUR C. Current understanding of ultrafine particulate matter emitted from mobile sources. J Air. Waste Manage. Assoc., **59** (1), 3, **2009**.
29. ZIELINSKA B., SAGEBIEL J., ARNOTT W.P., ROGERS C.F., KELLY K.E., WAGNER D.A., LIGHTY J.S., SAROFIM A.F., PALMER G. Phase and size distribution of polycyclic aromatic Hydrocarbons in diesel and gasoline vehicle emissions. Environ. Sci. Technol., **38** (9), 2557, **2004**.
30. KUMAR A., SINGH D., KUMAR K., SINGH B.B., JAIN V.K. Distribution of VOCs in urban and rural atmospheres of subtropical India: Temporal variation, source attribution, ratios, OFP and risk assessment. Sci. Total Environ., **613**, 492, **2018**.
31. GAO C., HE Z., LI J., LI X., BAI Q., ZHANG Z., ZHANG X., WANG S., XIAO X., WANG F., YAN Y., LI D., CHEN L., ZENG X., XIAO Y., DONG G., ZHENG Y., WANG Q., CHEN W. Specific long non-coding RNAs response to occupational PAHs exposure in coke oven workers. Toxicol. Reports, **3**, 160, **2016**.
32. LEVESQUE S., SURACE M.J., MCDONALD J., BLOCK M.L. Air pollution & the brain: Subchronic diesel exhaust exposure causes neuroinflammation and elevates early markers of neurodegenerative disease. J Neuroinflammation, **8** (1), 105, **2011**.